NANO LETTERS

2007
Vol. 7, No. 2
496−501

Plasmonic Enhancement of Molecular Fluorescence

Felicia Tam,[†,⊥] Glenn P. Goodrich,[§] Bruce R. Johnson,[||,⊥] and Naomi J. Halas*[,‡,||,⊥]

Department of Physics and Astronomy, Department of Chemistry, Department of Electrical and Computer Engineering, and The Laboratory for Nanophotonics, Rice University, 6100 Main Street, Houston, Texas 77005, and Nanospectra Biosciences, Inc., 8285 El Rio Street, Suite 150, Houston, Texas 77054

Received December 11, 2006; Revised Manuscript Received January 13, 2007

ABSTRACT

Metallic nanoparticles are known to dramatically modify the spontaneous emission of nearby fluorescent molecules and materials. Here we examine the role of the nanoparticle plasmon resonance energy and nanoparticle scattering cross section on the fluorescence enhancement of adjacent indocyanine green (ICG) dye molecules. We find that enhancement of the molecular fluorescence by more than a factor of 50 can be achieved for ICG next to a nanoparticle with a large scattering cross section and a plasmon resonance frequency corresponding to the emission frequency of the molecule.

Since Purcell first suggested in 1946 that spontaneous emission could be modified by resonant coupling to the external electromagnetic environment,[1] a wealth of fundamental research and technological innovation has arisen based on this effect. Amplified and inhibited spontaneous emission have been observed from single atoms coupled to resonant cavities,[2,3] semiconductor quantum wells integrated into microstructures,[4−6] photonic crystals,[7,8] and fluorophores near metal surfaces and nanoparticles.[9−15] Numerous devices based on modified spontaneous emission have been demonstrated, including single-photon sources for quantum cryptography,[16,17] surface plasmon enhanced LEDs,[18] and photonic crystal lasers.[19] Enhancement of molecular fluorescence is of great interest due to the widespread popularity of molecular-fluorescence-based measurements and devices in fields such as chemistry, molecular biology, materials science, photonics, and medicine. Applications as diverse as single molecule detection,[20] automated DNA sequencing,[21] and examination of circulation in the heart and retina[22] all rely directly on the inherent brightness of the molecular fluorophore for detection sensitivity. The ability to increase the emission of fluorophores used in these applications would greatly enhance the effectiveness of these as well as other fluorophore-based techniques.

One important strategy to achieve fluorescence enhancement is to utilize metallic nanoparticles, which are known to drastically alter the emission of vicinal fluorophores.[23,24] Metallic nanoparticles can influence the fluorescent emission of nearby molecules in several ways: by enhancing the optical intensity incident on the molecule through near field enhancement, by modifying the radiative decay rate of the molecule, and by increasing the coupling efficiency of the fluorescence emission to the far field through nanoparticle scattering. All these processes can be controlled by molecule−nanoparticle separation, nanoparticle size, and geometry. The geometry and size of the nanoparticle determine the properties of the localized surface plasmons it supports. At the plasmon resonance wavelength of a metallic nanoparticle, the light intensity in the near field of the nanoparticle (also known as the fringing field) is enhanced strongly relative to the incident optical wave. While fluorescence from a molecule directly adsorbed onto the surface of a metallic nanoparticle is strongly quenched,[12,25] at a distance of a few nanometers from the nanoparticles its fluorescence can be strongly enhanced. Molecular emission is also influenced by modification of the molecular radiative decay rate by the nearby metallic nanoparticle which alters the quantum yield of the molecule in a manner similar to the effect of a nearby macroscopic metallic surface.[11,23,26] Coupling of the fluorescent emission to the far field is also influenced by the scattering efficiency of the metallic nanoparticle.[24] Nanoparticle scattering is known to increase with nanoparticle size, but it is also strongly dependent upon the plasmon excitation, since the optical cross section of the nanoparticle on resonance is strongly enhanced relative to its off-resonance value. By studying the dependence on plasmon energy and nanoparticle scattering efficiency of the molecular fluores-

* Corresponding author. E-mail: halas@rice.edu.
[†] Department of Physics and Astronomy, Rice University.
[‡] Department of Electrical and Computer Engineering, Rice University.
[§] Nanospectra Biosciences, Inc.
[||] Department of Chemistry, Rice University.
[⊥] The Laboratory for Nanophotonics, Rice University.

10.1021/nl062901x CCC: $37.00
Published on Web 01/27/2007

cence enhancement by metallic nanoparticles, we can gain a more comprehensive understanding of this inherently nanoscale process. Increased understanding of this interaction will ultimately lead to design strategies for optimizing molecular fluorescence enhancement with adjacent metallic nanostructures, a highly useful goal with direct relevance in many molecule-based measurement or device applications.

Although there has been extensive research on fluorescence modification by nanoparticles, the role of the plasmon resonance energy with respect to the excitation and emission energies of a fluorophore is not well understood. Previous studies have focused primarily on solid Au or Ag nanoparticles.[27−29] Although the plasmon resonance of a solid metallic nanosphere can be red-shifted by increasing particle size, the scattering cross section of the nanoparticle will also increase, making it virtually impossible to examine each characteristic independently. Prior studies have also examined the enhancement of molecular fluorescence by polydisperse Ag nanorod films.[30] In general, research on this process has focused on high quantum yield fluorophores; however, fluorescence enhancement of low quantum yield fluorophores, converting poor emitters into good ones, may prove to be of far more practical significance.

To better examine the role of a nearby metallic nanoparticle's properties in the fluorescence enhancement of nearby molecules, we have studied the fluorescence emission of indocyanine green (ICG) in the vicinity of Au nanospheres and Au−silica nanoshells. This near-infrared-emitting dye is used extensively in clinical biomedical imaging diagnostics for determining cardiac output,[31] hepatic function, and blood flow[32] and for ophthalmic angiography.[33] Despite its extensive use, ICG is a remarkably weak fluorophore, with a quantum yield of only 1.2%.[34] Nanoshells are in many ways the optimal plasmonic nanoparticles for these experiments since their plasmon resonances are easily tuned across a large visible and infrared wavelength region by varying their internal geometry.[35−38] In the nanoshell geometry, the plasmon resonance energy, controlled by the ratio of the inner and outer radius of the metallic shell layer, can be varied independently of the nanoparticle scattering cross section which is controlled by absolute particle size. The spherical symmetry of this concentric layered nanostructure allows for straightforward experimental design as well as quantitative calculations of their plasmonic properties.[35,39−41]

Nanoshells of varying geometries were fabricated by seed-mediated electroless plating of Au onto silica spheres in a manner previously described.[42] Silica nanoparticle cores of 64 and 112 nm radii were synthesized using the Stöber method.[43] Larger 215 nm radius silica cores were obtained from Nissan Chemical, Inc. All nanoparticle sizes were monodisperse to within 10% standard deviation. Au colloid was prepared via reduction of $HAuCl_4$ by formaldehyde. Well-dispersed, submonolayer nanoparticle films were made by depositing the nanoparticles onto poly(vinylpyridine)-functionalized glass microscope slides as described previously.[44,45] Deposition of ICG onto the nanoparticle films was accomplished by immersion of the substrate in an aqueous 60 μM human serum albumin (HSA) solution for 2 h followed by a 1 h immersion in an aqueous solution of 30 μM ICG. HSA performs multiple functions in this experiment: it facilitates conjugation of the fluorophore to the nanoshell, acts as a 3.8−12 nm spacer layer to minimize quenching, and stabilizes the fluorophore by preventing ICG degradation.[46] The plasmonic properties of the nanoparticle substrates were characterized by extinction measurements using a Varian Cary 5000 UV−vis−NIR spectrometer. These samples were excited at 785 nm, well below saturation, and backscattered fluorescence emission was collected using a Renishaw micro-Raman spectrometer (Figure 1c, inset).

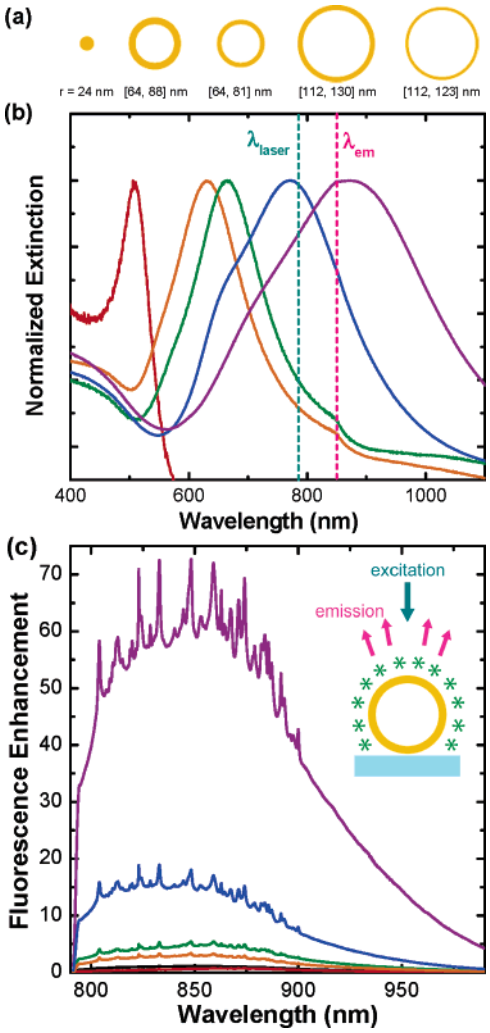

Figure 1. (a) Schematic of gold nanoparticles used as fluorescence enhancement substrates, arranged from short to long plasmon resonance wavelength. One Au colloid, and four nanoshells of various [r_1, r_2] were used. (b) Normalized extinction measurements from nanoparticle substrates corresponding to (a) in air prior to HSA and ICG deposition. The laser excitation is at 785 nm, and the emission wavelength of ICG attached to HSA is 850 nm. (c) Corresponding fluorescence emission from ICG conjugated to the nanoshell substrates adjusted for surface area available for fluorophore conjugation and normalized to the fluorescence from a control sample with no nanoparticles (black). Inset schematic illustrates experimental geometry.

Au nanoshells of four different sizes and geometries and one Au nanosphere preparation were used as substrates (Figure 1a). These sizes and geometries were specifically

chosen to span the wavelength region of excitation and emission of ICG. The far field extinction spectra of the nanoparticle substrates, prepared on a dielectric support in air ambient, are shown in Figure 1b. The corresponding fluorescence emission spectra from ICG−HSA on the nanoparticle substrates in Figure 1b are shown in Figure 1c. The fluorescence intensities have been normalized to the available surface area for fluorophore binding. The sharp, narrow features at the peak of the spectral fluorescence envelope correspond to surface-enhanced resonant Raman scattering[47] of the ICG molecules.[48] The intensity of the SERRS emission is proportional to the intensity of the broader underlying fluorescence emission. Fluorescence from the $r = 24$ nm nanosphere substrate showed a slight quenching relative to the emission intensities in the absence of a nanoparticle substrate, while the $[r_1, r_2] = [64, 81]$ nm and [64, 88] nm nanoshells showed relatively small enhancements. These smaller nanoparticles possess plasmon resonances detuned from the peak absorption and emission wavelengths of the molecule. While the fluorescence enhancements from the larger $[r_1, r_2] = [112, 123]$ nm and [112, 130] nm nanoshells surpassed those of the smaller nanoshells, the enhancements from these nanoshells are conspicuously different. The $[r_1, r_2] = [112, 130]$ nm nanoshell has a plasmon resonance tuned to the fluorophore excitation wavelength, creating the greatest near field enhancement of the nanoparticles studied, and produces an enhancement factor of approximately 15. By far the strongest enhancement factor of 50 is achieved with the $[r_1, r_2] = [112, 123]$ nm nanoshell, whose plasmon resonance overlaps with the ICG emission wavelength. From this observation, it appears that the fluorescence enhancement of a nanoparticle substrate is optimal when the nanoparticle plasmon resonance is tuned to the emission wavelength of the molecular fluorophore.

Since the nanoparticles used in this study vary significantly in size, we can also examine the role of scattering cross section and radiative rate enhancement in the fluorescence enhancement process. Here we can exploit the fact that the spherical symmetry of these nanoparticles allows us to calculate many of their properties quite straightforwardly, providing a qualitative theoretical understanding of our experimental observations. We calculated the angular scattering intensities of the nanoparticle substrates at the peak emission wavelength of the fluorophore (850 nm) using Mie scattering theory.[49] The normalized scattering characteristics as a function of polar angle are shown in Figure 2. These calculations show that the smaller nanoparticles, the $r = 24$ nm nanospheres and the $[r_1, r_2] = [64, 81]$ nm and [64, 88] nm nanoshells, scatter far less efficiently than the $[r_1, r_2] = [112, 123]$ nm and [112, 130] nm nanoshells, due to both the differences in their sizes and plasmon resonances. Therefore, the difference in scattering efficiency can account for the greater fluorescence enhancement from the larger nanoshells. However, they also show that the scattering from the two $r_1 = 112$ nm nanoshells is approximately equivalent, although experimentally the $[r_1, r_2] = [112, 123]$ nm nanoshell substrates were observed to yield a fluorescence

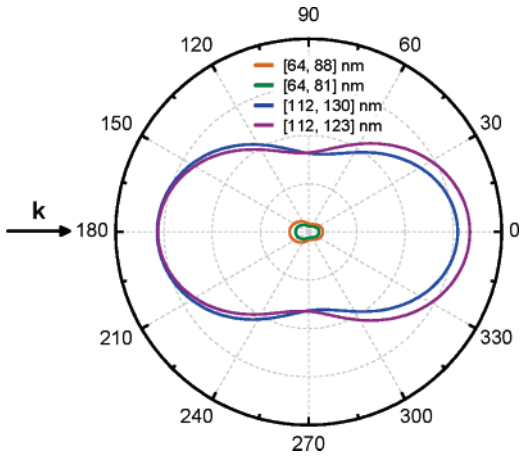

Figure 2. Calculated normalized angular scattering intensity at 850 nm from nanoparticles in a uniform dielectric medium of $n = 1$. The radial axis scale ranges from 0 to 2. The scattering from $r = 24$ nm colloid is too small to be visible on this scale.

enhancement for ICG four times greater than the $[r_1, r_2] = [112, 130]$ nm nanoshell substrates. These calculations indicate that although the nanoparticle scattering efficiency plays a role in the observed fluorescence enhancement, scattering efficiency alone does not entirely account for the differences in enhancement factors observed experimentally across the various nanoparticle geometries.

Another mechanism contributing to fluorescence enhancement is the nanoparticle modification of a fluorophore's radiative and nonradiative decay rates.[12,23,24] For the spherical nanoshell geometry, the radiative rate enhancement χ_r can be calculated[50] in a manner that directly parallels the previously obtained treatment for solid metallic spheres[51,52]

$$\chi_r = \frac{3}{2p^2}\sum_{l=1}^{\infty}(2l+1)\left\{p_r^2 l(l+1)(k_S r)^{-2}\left|j_l(k_S r) + b_l h_l^{(1)}(k_S r)\right|^2 + \frac{p_\theta^2 + p_\phi^2}{2}\left[|j_l(k_S r) + a_l h_l^{(1)}(k_S r)|^2 + |\eta_l^j(k_S r) + b_l \eta_l^h(k_S r)|\right]^2\right\}$$

where

$$\eta_l^h(x) = \frac{1}{x}\frac{d}{dx}x h_l^{(1)}(x)$$

$$\eta_l^j(x) = \frac{1}{x}\frac{d}{dx}x j_l(x)$$

and a_l and b_l are coefficients of the vector spherical harmonic expansion of the scattered electromagnetic field,[53] p is the transition dipole moment $p = (p_r, p_\theta, p_\phi)$, l is the angular momentum quantum number, r is the location of the dipole with respect to the nanoparticle center, k_S is the scattered wavevector, and $h_l^{(1)}$ and j_l are the spherical Hankel and Bessel Functions, respectively. Calculated radiative rate enhancements for a fluorophore situated near nanoshells with

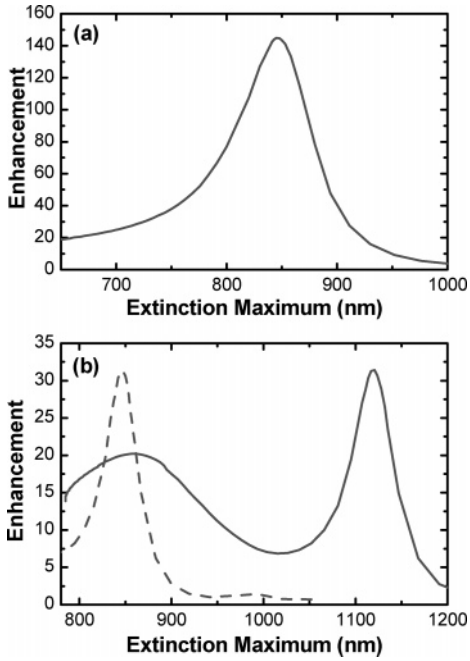

Figure 3. Calculated radiative rate enhancements as a function of the nanoparticle plasmon resonance wavelength in a homogeneous dielectric medium of air. Enhancement maxima occur when either the dipole (solid) or quadrupole (dashed) plasmon excitation of the nanoparticle corresponds with the emission wavelength of the fluorophore at 850 nm. (a) Calculated enhancements on nanoshells with a $r_1 = 64$ nm and varying values of r_2. (b) Calculated enhancements on nanoshells with $r_1 = 112$ nm and various values of r_2.

$r_1 = 64$ and 112 nm and varying r_2 (corresponding to different plasmon resonances) are shown in Figure 3. A maximal coupling between the fluorophore and nanoparticle is assumed in these calculations, corresponding to a fluorophore−nanoparticle separation of 3.8 nm (the smallest dimension of the HSA spacer molecules) and an ICG dipole moment oriented perpendicular to the particle surface.

Slight differences in experimental geometry with respect to theory (nanoparticles on dielectric substrate versus a homogeneous dielectric environment) prevent quantitative comparison between experimental observations and theoretical analysis.[45,54] However, this analysis indicates that there is a clear theoretical correlation between the plasmon resonance wavelength and the maximum radiative rate enhancement of the fluorophore. In both cases, the radiative rate enhancement is maximal when either the dipole or the quadrupole resonance of the nanoshell corresponds to the maximum emission wavelength of the fluorophore at 850 nm. (The plasmon resonances of Au nanospheres cannot be tuned to 850 nm for experimentally feasible sizes.) On the basis of this analysis, it is quite likely that the difference in the observed fluorescence enhancement of ICG on the [r_1, r_2] = [112,123] nm and [112, 130] nm nanoshells is due to a difference in radiative rate enhancement in the ICG layers induced by the nanoparticles.

On the basis of this analysis, we can ask the following question: Is it possible to change the fluorescence enhancement of a plasmonic nanoparticle substrate by tuning the plasmon resonance using another mechanism? This should be possible in principle, since the plasmon resonance influences both the radiative rate enhancement and the nanoparticle scattering efficiency. Therefore, any mechanism, external or internal, that tunes the plasmon resonance of a nanoparticle should influence its enhancement of nearby fluorophores. It is well-known that the plasmon resonance energy of a nanoparticle can be strongly shifted by changes in its dielectric environment.[45,55,56] Monitoring the changes in fluorescence enhancement that occur as the refractive index of the surrounding medium is varied allows us to systematically shift the nanoparticle substrate resonance frequencies while maintaining nanoparticle size, geometry, fluorophore orientation, and surface coverage. In each dielectric medium the relative fluorescence enhancements due to the plasmon resonance energy should vary systematically (however, absolute fluorescence enhancement variations as a function of differing dielectric environments are not directly comparable due to differences in optical collection efficiencies and fluorescent lifetimes in various media.

Nanoshell substrates with three nanoparticle geometries were fabricated such that their plasmon resonances were close to resonant with the fluorophore in either air or water (Figure 4). The plasmon resonance of each nanoshell shifts to longer wavelengths as the dielectric medium surrounding the nanoshell increases from $n = 1$ in air to $n = 1.33$ in water (Figure 4a).[45,55,57] The [r_1, r_2] = [215, 231] nm nanoshell exhibits the greatest plasmon shift upon changes in solvent refractive index due to its significantly larger size.[45] Fluorescence emission from ICG conjugated to these substrates in air shows the greatest fluorescence enhancement with the [r_1, r_2] = [215, 231] nm nanoshell (Figure 4b), which has the plasmon resonance closest to the ICG emission wavelength in air as well as the greatest backscattering efficiency (Figure 4b, inset). When these same substrates are immersed in water, in addition to plasmon resonance shifts, the scattering properties also change as the size of the nanoparticles increases relative to the wavelength of incident light in the new dielectric. The backscattering efficiencies of all the nanoshells are roughly equivalent in water (Figure 4c, inset), leaving only variations in radiative rate enhancement to cause differences in fluorescence enhancement. As a result, the fluorescence enhancements increase with the proximity of the plasmon resonances in water to the emission wavelength of ICG: the [r_1, r_2] = [64, 81] nm nanoshell shows the greatest fluorescence enhancement, followed by the [r_1, r_2] = [64, 88] nm nanoshell and then the [r_1, r_2] = [215, 231] nm nanoshell. These results indicate that the ability of a nanoparticle to enhance the fluorescence emission of a nearby fluorophore can be drastically altered by changing the plasmon resonance energy and scattering properties of a nanoparticle through changes in its dielectric surroundings.

In conclusion, we have shown that plasmonic nanoparticle-based fluorescence enhancement of a low quantum yield molecular fluorophore is strongly influenced by the plasmon resonance energy of the nanoparticle and its scattering efficiency. Both experimental observations and theoretical

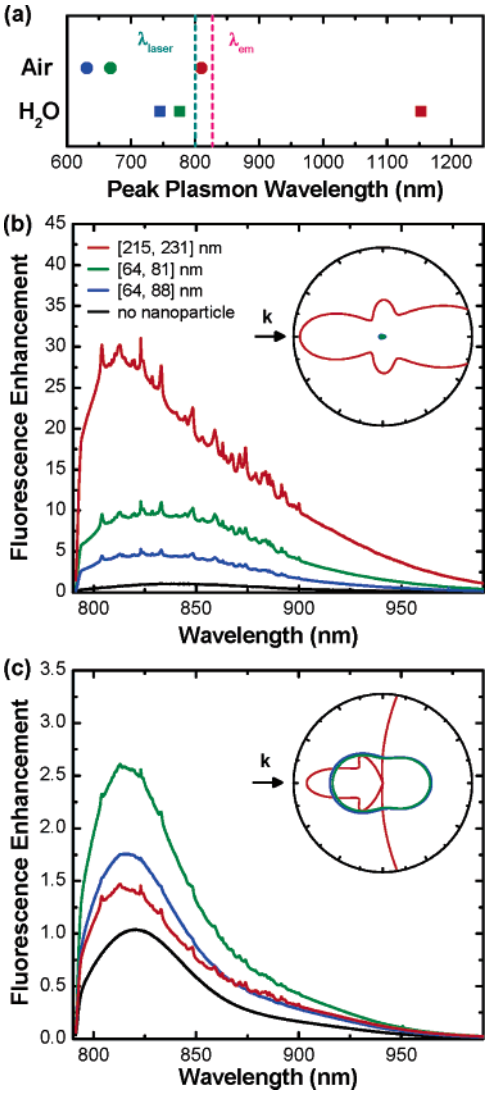

Figure 4. (a) Plasmon resonance wavelength of nanoshell substrates of various [r_1, r_2] in both air and water. (b) Fluorescence emission from the ICG conjugated to the nanoshell substrates from (a) in air, normalized to the control sample with no nanoshells (black). Inset shows normalized scattering efficiency for the nanoparticles. (c) Normalized fluorescence emission and scattering (inset) from the same samples in water.

analysis involving nanoparticles of different plasmon resonance energies and scattering properties show that fluorescence enhancement is optimized by increasing particle scattering efficiency while tuning the plasmon resonance to the emission wavelength of the fluorophore. An increased understanding of the interaction between plasmonic nanoparticles and excited-state molecules should make it possible to design nanoparticle−molecule complexes that optimally enhance the emission of any given fluorophore.

Acknowledgment. This work was supported by the Air Force Office of Scientific Research Grant FA9550-06-1-0021, the National Science Foundation (NSF) Grants EEC-0304097 and CHE-0518476, the Robert A. Welch Foundation C-1220, and the Multidisciplinary University Research Initiative (MURI) Grant W911NF-04-01-0203.

References

(1) Purcell, E. M. *Phys. Rev.* **1946**, *69* (11−1), 681−681.
(2) Goy, P.; Raimond, J. M.; Gross, M.; Haroche, S. *Phys. Rev. Lett.* **1983**, *50* (24), 1903−1906.
(3) Hulet, R. G.; Hilfer, E. S.; Kleppner, D. *Phys. Rev. Lett.* **1985**, *55* (20), 2137−2140.
(4) Gerard, J. M.; Sermage, B.; Gayral, B.; Legrand, B.; Costard, E.; Thierry-Mieg, V. *Phys. Rev. Lett.* **1998**, *81* (5), 1110−1113.
(5) Gerard, J. M.; Gayral, B. *J. Lightwave Technol.* **1999**, *17* (11), 2089−2095.
(6) Kiraz, A.; Michler, P.; Becher, C.; Gayral, B.; Imamoglu, A.; Zhang, L. D.; Hu, E.; Schoenfeld, W. V.; Petroff, P. M. *Appl. Phys. Lett.* **2001**, *78* (25), 3932−3934.
(7) Yablonovitch, E. *Phys. Rev. Lett.* **1987**, *58*, 2059−2062.
(8) Boroditsky, M.; Vrijen, R.; Krauss, T. F.; Coccioli, R.; Bhat, R.; Yablonovitch, E. *J. Lightwave Technol.* **1999**, *17* (11), 2096−2112.
(9) Drexhage, K. H. *J. Lumin.* **1970**, *1*, 2, 693−701.
(10) Gontijo, I.; Boroditsky, M.; Yablonovitch, E.; Keller, S.; Mishra, U. K.; DenBaars, S. P. *Phys. Rev. B* **1999**, *60* (16), 11564−11567.
(11) Chance, R. R.; Prock, A.; Silbey, R. *J. Chem. Phys.* **1974**, *60* (7), 2744−2748.
(12) Dulkeith, E.; Morteani, A. C.; Niedereichholz, T.; Klar, T. A.; Feldmann, J.; Levi, S. A.; van Veggel, F.; Reinhoudt, D. N.; Moller, M.; Gittins, D. I. *Phys. Rev. Lett.* **2002**, *89* (20), 203002.
(13) Kummerlen, J.; Leitner, A.; Brunner, H.; Aussenegg, F. R.; Wokaun, A. *Mol. Phys.* **1993**, *80* (5), 1031−1046.
(14) Weitz, D. A.; Garoff, S.; Hanson, C. D.; Gramila, T. J.; Gersten, J. I. *J. Lumin.* **1981**, 24−5 (NOV), 83−86.
(15) Biteen, J. S.; Lewis, N. S.; Atwater, H. A.; Mertens, H.; Polman, A. *Appl. Phys. Lett.* **2006**, *88*, (13), 131109.
(16) Pelton, M.; Santori, C.; Vuckovic, J.; Zhang, B. Y.; Solomon, G. S.; Plant, J.; Yamamoto, Y. *Phys. Rev. Lett.* **2002**, *89* (23), 233602.
(17) Waks, E.; Inoue, K.; Santori, C.; Fattal, D.; Vuckovic, J.; Solomon, G. S.; Yamamoto, Y. *Nature* **2002**, *420* (6917), 762−762.
(18) Vuckovic, J.; Loncar, M.; Scherer, A. *IEEE J. Quantum Electron.* **2000**, *36* (10), 1131−1144.
(19) Painter, O.; Lee, R. K.; Scherer, A.; Yariv, A.; O'Brien, J. D.; Dapkus, P. D.; Kim, I. *Science* **1999**, *284* (5421), 1819−1821.
(20) Weiss, S. *Science* **1999**, *283* (5408), 1676−1683.
(21) Pease, A. C.; Solas, D.; Sullivan, E. J.; Cronin, M. T.; Holmes, C. P.; Fodor, S. P. A. *Proc. Natl. Acad. Sci. U.S.A.* **1994**, *91* (11), 5022−5026.
(22) Frangioni, J. V. *Curr. Opin. Chem. Biol.* **2003**, *7*, (5), 626−634.
(23) Barnes, W. L. *J. Mod. Opt.* **1998**, *45* (4), 661−699.
(24) Lakowicz, J. R. *Anal. Biochem.* **2005**, *337* (2), 171−194.
(25) Anger, P.; Bharadwaj, P.; Novotny, L. *Phys. Rev. Lett.* **2006**, *96*, (11).
(26) Drexhage, K. H.; Kuhn, H.; Schafer, F. P. *Ber. Bunsen-Ges. Phys. Chem.* **1968**, *72* (2), 329-&.
(27) Sokolov, K.; Chumanov, G.; Cotton, T. M. *Anal. Chem.* **1998**, *70* (18), 3898−3905.
(28) Kulakovich, O.; Strekal, N.; Yaroshevich, A.; Maskevich, S.; Gaponenko, S.; Nabiev, I.; Woggon, U.; Artemyev, M. *Nano Lett.* **2002**, *2* (12), 1449−1452.
(29) Kuhn, S.; Hakanson, U.; Rogobete, L.; Sandoghdar, V. *Phys. Rev. Lett.* **2006**, *97* (1), 017402.
(30) Aslan, K.; Leonenko, Z.; Lakowicz, J. R.; Geddes, C. D. *J. Phys. Chem. B* **2005**, *109* (8), 3157−3162.
(31) Iijima, T.; Aoyagi, T.; Iawo, Y.; Masuda, J.; Fuse, M.; Kobayashi, N.; Sankawa, H. *J. Clin. Monit.* **1997**, *13*, 81−89.
(32) Tsubono, T.; Todo, S.; Jabbour, N.; Mizoe, A.; Warty, V.; Demetris, A. J.; Starzl, T. E. *Hepatology* **1996**, *24*, 1165−1171.
(33) Dzurinko, V. L.; Gurwood, A. S.; Price, J. R. *Optometry* **2004**, *75*, 743−755.
(34) Benson, R. C.; Kues, H. A. *Phys. Med. Biol.* **1978**, *23*, 159−163.
(35) Averitt, R. D.; Sarkar, D.; Halas, N. J. *Phys. Rev. Lett.* **1997**, *78* (22), 4217−4220.
(36) Oldenburg, S. J.; Averitt, R. D.; Westcott, S. L.; Halas, N. J. *Chem. Phys. Lett.* **1998**, *288* (2−4), 243−247.
(37) Oldenburg, S. J.; Jackson, J. B.; Westcott, S. L.; Halas, N. J. *Appl. Phys. Lett.* **1999**, *75* (19), 2897−2899.
(38) Prodan, E.; Nordlander, P. *Nano Lett.* **2003**, *3*, 543−547.
(39) Prodan, E.; Nordlander, P. *J. Chem. Phys.* **2004**, *120*, 5444−5454.
(40) Prodan, E.; Lee, A.; Nordlander, P. *Chem. Phys. Lett.* **2002**, *360*, 325−332.
(41) Oubre, C.; Nordlander, P. *J. Phys. Chem. B* **2004**, *108*, 17740−17747.

(42) Oldenburg, S. J.; Westcott, S. L.; Averitt, R. D.; Halas, N. J. *J. Chem. Phys.* **1999**, *111* (10), 4729−4735.
(43) Stober, W.; Fink, A.; Bohn, E. *J. Colloid Interface Sci.* **1968**, *26* (1), 62−69.
(44) Malynych, S.; Luzinov, I.; Chumanov, G. *J. Phys. Chem. B* **2002**, *106* (6), 1280−1285.
(45) Tam, F.; Moran, C.; Halas, N. *J. Phys. Chem. B* **2004**, *108* (45), 17290−17294.
(46) Hollins, B.; Noe, B.; Henderson, J. M. *Clin. Chem.* **1987**, *33* (6), 765−768.
(47) Kneipp, K.; Kneipp, H.; Itzkan, I.; Dasari, R. R.; Feld, M. S. *Chem. Rev.* **1999**, *99*, (10), 2957−2976.
(48) Kneipp, J.; Kneipp, H.; Rice, W. L.; Kneipp, K. *Anal. Chem.* **2005**, *77* (8), 2381−2385.
(49) Mie, G. *Ann. Phys.* **1908**, *24*, 377.
(50) Gibson, J. W.; Johnson, B. R. *J. Chem. Phys.* **2006**, *124* (6), 064701.
(51) Chew, H. *J. Chem. Phys.* **1987**, *87*, 1355−1360.
(52) Kerker, M.; Wang, D.-S.; Chew, H. *Appl. Opt.* **1980**, *19*, 4159−4174.
(53) Aden, A. L.; Kerker, M. *J. Appl. Phys.* **1951**, *22*, 1242.
(54) Sherry, L. J.; Chang, S. H.; Schatz, G. C.; Van Duyne, R. P.; Wiley, B. J.; Xia, Y. N. *Nano Lett.* **2005**, *5* (10), 2034−2038.
(55) Jensen, T. R.; Duval, M. L.; Kelly, K. L.; Lazarides, A. A.; Schatz, G. C.; Van Duyne, R. P. *J. Phys. Chem. B* **1999**, *103* (45), 9846−9853.
(56) Sun, Y.; Xia, Y. *Anal. Chem.* **2002**, *74*, 5297−5305.
(57) Templeton, A. C.; Pietron, J. J.; Murray, R. W.; Mulvaney, P. *J. Phys. Chem. B* **2000**, *104* (3), 564−570.

NL062901X